Naval Research Laboratory
Washington, DC 20375-5320

NRL/MR/6730--00-8420

Temporal Steadiness and Its Control in Laser Driven Shocks

A.N. Mostovych

Laser Plasma Branch
Plasma Physics Division

E.A. McLean

Research Support Instruments, Inc.
4325 Forbes Boulevard, Suite B
Lanham, MD

L. Phillips

Center for Computational Physics Developments
Laboratory for Computational Physics and Fluids Dynamics

T. Lehecka
A.V. Deniz

Science Applications International Corporation
McLean, VA

December 29, 2000

20010227 125

REPORT DOCUMENTATION PAGE

1. AGENCY USE ONLY (Leave Blank)	2. REPORT DATE	3. REPORT TYPE AND DATES COVERED
	December 29, 2000	Memorandum Report 1998-1999

4. TITLE AND SUBTITLE

Temporal Steadiness and Its Control in Laser Driven Shocks

5. FUNDING NUMBERS

6. AUTHOR(S)

A.N. Mostovych, E.A. McLean,* L. Phillips, T. Lehecka,** and A.V. Deniz**

7. PERFORMING ORGANIZATION NAME(S) AND ADDRESS(ES)

Naval Research Laboratory
Washington, DC 20375-5320

8. PERFORMING ORGANIZATION REPORT NUMBER

NRL/MR/6730--00-8420

9. SPONSORING/MONITORING AGENCY NAME(S) AND ADDRESS(ES)

Department of Energy
1301 Clay Street
Oakland, CA 94612

10. SPONSORING/MONITORING AGENCY REPORT NUMBER

12a. DISTRIBUTION/AVAILABILITY STATEMENT

Approved for public release; distribution is unlimited.

12b. DISTRIBUTION CODE

13. ABSTRACT (Maximum 200 words)

The time dependence of laser driven shocks is studied in a series of experiments on multiply-stepped solid aluminum targets, using ISI smoothed laser profiles and variable shaped temporal laser pulses. The shock speed depends upon the laser pulse shape, the target thickness, and the material properties at the ablation surface. Comparisons with hydro-code calculations show good agreement to within 2% for steady-state shocks whereas comparison for non-steady shocks vary up to 40%.

14. SUBJECT TERMS

Laser driven shocks
Equation of State (EOS)

15. NUMBER OF PAGES

18

16. PRICE CODE

17. SECURITY CLASSIFICATION OF REPORT	18. SECURITY CLASSIFICATION OF THIS PAGE	19. SECURITY CLASSIFICATION OF ABSTRACT	20. LIMITATION OF ABSTRACT
UNCLASSIFIED	UNCLASSIFIED	UNCLASSIFIED	UL

Laser driven shock waves can readily produce pressures in the laboratory of up to 100Mbar. This provides the potential for equation-of-state (EOS) studies under pressure conditions not previously attainable in the laboratory. With the development of high power lasers in the 1970s', high pressures were quickly demonstrated by various experiments[1,2], but experiments capable of accurate EOS measurements have only been reported[3,4,5] recently. Typical difficulties have included edge effects from the small laser illumination area, spatial and temporal non-uniformities in the laser pulse, and target preheat.

Basic shock properties such as the shock and mass flow velocities of 1-dimensional planar shocks are directly related to the EOS (E=f(P,V)) through the Rankine-Hugoniot relations:

$$P - P_o = \frac{u_s u_p}{V_o} \tag{1}$$

$$V = V_o\left(1 - \frac{u_p}{u_s}\right) \tag{2}$$

$$E - E_o = \frac{1}{2}(P + P_o)(V_o - V) \tag{3}$$

where P, V, and E are the pressure, volume, and total energy behind the shock, where u_s and u_p denote the shock and particle flow velocities, and where P_o, V_o, and E_o are the initial conditions. A complete knowledge of the state variables in the final shock state is obtained from an independent measurement of any two of the variables. These relations are valid for steady and non-steady shocks as long as the shock front is discontinuous. If the shock is non-steady the Rankine-Hugoniot relations relate the instantaneous and not the average state variables in front and behind the shock front. This imposes a severe restriction on the accuracy of laser EOS

experiments because measurements of instantaneous shock properties in these experiments are prone to large errors. The importance of these uncertainties is estimated by considering the propagation of errors in the Rankine-Hugoniot relations. For the case were the shock velocity and particle velocity are measured with uncertainties $\Delta u_s / u_s$ and $\Delta u_p / u_p$, the expected error in the density is given by $\Delta \rho / \rho \sim (\rho/\rho_0 - 1)\{(\Delta u_s / u_s)^2 + (\Delta u_p / u_p)^2 + 2\sigma^2_{sp}(\Delta u_s / u_s)(\Delta u_p / u_p)\}^{1/2}$, where σ^2_{sp} is the covariance between u_s and u_p. As an example, Al shocked to 10 Mbars undergoes a compression of $\rho/\rho_0 \sim 2.65$ and will require an accuracy of about 2% in the velocity measurements to give an overall 5% accuracy in the density determination. If the shock is also unsteady with a 2% change in velocity over the time of the measurement then the overall accuracy can further degrade to about 10%. Materials undergoing higher shock compression will have even larger errors, $\sim 18\%$ for $\rho/\rho_0 = 4$, as in an ideal gas. In some cases errors may partially cancel as a result of negative covariance terms but in general measurements of EOS properties to within 10% will require shocks that are steady to better than 2%.

Laser produced shocks are often not steady because of time variations of the laser drive pulse and because of the dynamics of the laser-target ablation physics. The processes responsible for these variations, are thought to be well understood, have been modeled analytically,[6] and are routinely calculated by various hydrodynamic codes. Unfortunately, systematic and accurate data are not readily available to evaluate the capability of our models and codes to predict the temporal behavior of unsteady shocks. In this work, we report on laser shock experiments with sufficient accuracy and time duration to study the temporal behavior of shocks as a function of the laser drive pulse shape, target thickness, and material properties of the ablation surface. These issues are of key importance in designing, interpreting, and validating laser-shock EOS measurements.

We find that it is difficult but possible to obtain steady state shocks in the 2% range that is required for accurate EOS measurements

We use the Nike KrF laser, with laser beams that are optically smoothed by Induced Spatial Incoherence (ISI), to generate very smooth illumination profiles on target ($\delta I/I < .02$) and to drive well-controlled planar shocks.[7] As per Fig. 1, the multiple beams (20-44 beams,~50 Joules/beam) of the NIKE laser are focused to a ~750 μm spot on a planar aluminum target with an intensity of 10^{13}-10^{14} w/cm^2. A thin layer of CH plastic is deposited on the target surface to lower the average Z, thus minimizing x-radiation output and target preheat. The rear surface of the target is micro-machined to produce several steps. The different shock propagation times through the steps are recorded with an optical streak camera which detects the light emission from the high temperature shocks as they break out of the rear of the target. Typically, the target has an aluminum base of about 30-60 μm, two or three additional 20μm steps, and 10μm CH ablation layer. Target metrology is performed with white light interferometry, giving a step height accuracy of $\pm$ 0.1 μm. The streak camera is independently calibrated with a set of short laser pulses (~10 ps) multiply reflected between two mirrors. These calibration measurements give a typical streak camera accuracy of $\pm$10 ps for relative time measurements in a single streak record.

The streaked emission record from a typical shock through a two step target is displayed on the right in Fig. 1. A planar shock is shown emerging from both sides of the steps. The shock break-out from the 1st and 2nd steps occur after delays of ~1ns. For targets up to 100 μm in thickness the shock is found to be uniform over the central 400-450 μm of the 750 μm laser profile. Accordingly, the step widths (100 μm for two steps and 75 μm for three steps) are chosen to insure that the steps are well inside the central uniform region but wide enough to

mitigate edge effects. In the worst case, the shock release from the step edges is not expected to move sideways more than the 20 μm thickness of the steps.[8] The rise-time of the emission signal is typically 20-30 ps, primarily limited by the time response of the streak camera. The shock break-out time is determined from a spatially averaged (~25μm) line-out profile of this emission signal. See Fig. 2. The emission characteristics of a shock signal are complicated at the foot and at the peak of the emission profile. To avoid complications in the definition of the shock arrival time, we define the shock break-out time as the mid-point of the least-squares line-fit to the steepest portion of the emission profile. This definition is meant to be used for relative measurements of shock arrival time at the different steps of a target in a single experiment. It may be different than the true arrival time of the shock but because the shock strength is relatively constant in these experiments, this difference should remain constant and cancel in a relative measurement.

The shock breakout time as a function of shock position at the various step heights is used to determine the shock speed and its history. In this experiment there are three primary variables: the laser pulse shape, the target thickness and the presence or absence of a CH layer on the laser-side of the target. Fig. 3. shows data where the experimental parameters are optimized for steady shock propagation. The temporal pulse shape of the laser is flat-topped, as in the insert. The target has a 10μm CH preheat layer. The target base is much thicker (60μm) than the thickness of the CH layer and the distance over which start-up transients dissipate. The shock is steady and propagates with a velocity of 2.2×10^6 cm/s (P ~ 7 Mbar). The error bars for each data point are smaller than the size of the data symbol (~ 20 ps and 0.2 μm). For shaped pulses, in Fig. 4, the shock propagation is substantially less steady. For this case the target thickness and the CH

preheat layer are held constant while the laser is modified to produce a fast-rise, fast-fall, and long-tail pulse, as in the insert. The driving pressure falls with the laser pulse and the shock-speed decays by more than 20% in the last steps in the target. The decay in shock speed is observed at a time commensurate ($\Delta t \sim 1.5$nsec) with the propagation of a rarefaction wave from the front surface that began with the fall in the laser pulse. Strong shock decay is also observed, in Fig. 5, for the case where the target base thickness is reduced to about 30μm while the laser pulse is held steady. With this thinner target, the shock is still evolving as a result of initial ablation-driven pressure transients and because of shock reflections at the Al-CH interface. For the case where the targets had no CH ablation layer, in Fig. 6, it was not possible to obtain a steady shock, regardless of the shape of the laser pulse or the thickness of the target. Calculations show that radiation form the laser-side of a pure aluminum target increases and heats the target interior to the point that the target steps expand and affect the shock measurement.

The experimental data are used to evaluate the capability of NRL's FAST2D laser-matter interaction code[9] to accurately predict the temporal behavior of planar shocks under varying experimental conditions. The experiments are modeled with the one-dimensional, planar version of the code. It uses a moving-grid semi-Eulerian numerical formulation that allows the computational grid to track the moving ablation surface. The hydrodynamic equations are solved using the Flux Corrected Transport (FCT) algorithm,[10] which was developed for solving problems involving sharp gradients, such as shocks, with high accuracy and minimal numerical diffusion. The accuracy and suitability of FCT for shock-propagation problems was verified with analytical benchmarks.[11] The ablation of the solid materials by the laser, their ionization, and the interaction of the laser with the blowoff plasmas are all included in the calculation. The code also

includes radiation transport through the use of lookup tables of atomic opacities. The calculations are done on 0.3μm grid and use an adjustable time step, ranging between 0.1ps and 1 ps. In Figs. 3 to 6, the curves through the data show specific calculations for the conditions of each shot. To allow for absolute timing errors and uncertainties in the laser intensity (± 20%), the time origin (T=0) of the data and the calculation are set to the time that the shock first breaks out of the base layer. Shock velocities are obtained by differentiating the measured and calculated shock trajectories. Typically, differentiation introduces additional numerical noise but the shock velocities are well represented by an average slowly varying curve. For conditions with flat-topped laser pulses and thick CH coated targets, the code calculations agree with the experiment, Fig. 3, predicting a very steady shock. The velocity plot shows the shock velocity decaying linearly. The best fit to the data gives a decay of only 1% per nsec as the shock propagates through the stepped region of the target. The difference between the slope of a linear fit to the measured and calculated data is less than 1%. For the cases with thinner targets, targets without the CH ablation layer, or with structured laser pulses, the agreement with calculations is not as good. In these cases, the calculations predict the shocks to be more steady than is observed in the experiment. This is not due to uncertainties in the laser intensity. A variation of the average laser intensity in the calculation by ±20% moves the point of intersection between the data and calculated velocity curves by less than ±10% and does not change the difference in slope. The discrepancies between the code calculations and the experiment are the greatest when the initial pressure transients are enhanced by structured laser pulses or where the initial pressure transients do not have sufficient time to dissipate as a result of short propagation times in thin targets. This suggests that the details of how the initial transients are treated in the calculations and the degree to which the laser intensity is known in the sharply changing laser pulse are very important for

Mostovych *et al.*

obtaining good comparison between the code and experiment. At this point it is not clear if the observed discrepancies result from difficulties in determining the exact pulse shape of a multi-beam high power laser or from difficulties in modeling the initial breakdown of the target as it transitions from a solid to a high temperature plasma.

In summary, the propagation of planar laser-driven shock waves has been measured with high accuracy in stepped aluminum targets. For the best conditions, the shock velocity is uniform within ±2%, a regime that is conducive to equation-of-state measurements. The shock velocity is sensitive to changes in the temporal pulse shape of the laser, to the position within the target, and to target preheat. Computer simulations accurately predict asymptotic shock behavior but do not match the experiment for the early times when the pressure undergoes rapid changes. As a result, high accuracy equation-of-state experiments will require verified steady-state behavior.

References:

[1] L.R. Veeser and J.C. Solem, Phys. Rev. Lett. **40**, 1391 (1978).

[2] R. J. Trainor, J. W. Shaner, J. M. Auerbach, and N. C. Holmes, Phys. Rev. Lett. **42**, 1154 (1979).

[3] A. Benuzzi, T. Löwer, M. Koenig, B. Faral, D. Batani, D. Beretta, C. Danson, and D. Pepler, Phys. Rev. E **54**, 2162 (1996).

[4] A. M. Evans, N. J. Freeman, P. Graham, C. J. Horsfield, S. D. Rothman, B. R. Thomas, and A. J. Tyrrell, Laser Part. Beams **14**, 113 (1996).

[5] Sizu Fu, Yuan Gu, Jiang Wu, and Shiji Wang, Phys. Plasmas **2**, 3461 (1995).

[6] R. J. Trainor and Y. T. Lee, Phys. Fluids **25**, 1898 (1982).

[7] S. P. Obenschain, S. E. Bodner, D. Colombant, K. Gerber, R. H. Lehmberg, E. A. McLean, A. N. Mostovych, M. S. Pronko, C. J. Pawley, A. J. Schmitt, J. D. Sethian, V. Serlin, J. A. Stamper, C. A. Sullivan, J. P. Dahlburg, J. H. Gardner, Y. Chan, A. V. Deniz, J. Hardgrove, T. Lehecka, and M. Klapisch, Phys. Plasmas **3**, 2098 (1996).

[8] Edge effects can not move faster than the shock. Instead, they will move in at roughly the sound speed behind the shock. Ya. B. Zeldovich and Yu. P. Raizer, *Physics of Shock Waves and High-Temperature Hydrodynamic Phenomena*, (Academic Press, New York, 1964).

[9] J. Gardner and S. Bodner, Phys. Fluids **29**, 2672 (1986).

[10] J. P. Boris, and D. L. Book, Methods in Computational Physics, **16**, 85 (1976)

[11] J. P. Boris, A. M. Landsberg, E. S. Oran, and J. H. Gardner, NRL Memo report 6410-93-7192, (1993)

Figure Captions:

Fig. 1. Schematic of experiment and sample streak photograph of shocked target. Target steps on target rear delay shock arrival time. The target has a 10μm CH ablation layer, a 60μm base, and is driven by a 4nsec flat laser pulse.

Fig. 2. Typical emission profile that is produced by a shock breaking out of the rear of a 60μm target. The target has a 10μm CH ablation layer and is driven by a 4nsec flat laser pulse. Data corresponds to a 25μm spatial average. Shock time is defined as the mid-point of the fit to the steepest portion of the profile.

Fig. 3. Measurements of shock position inside the target as a function of breakout time. The combination of a steady laser pulse, thick target base, and a low-radiation CH ablation layer are necessary to produce shocks sufficiently steady for EOS studies. Curve through the data due to 1d hydrodynamic simulations

Fig. 4. Structured laser pulses are used to test the sensitivity of shocks to changes in the ablation pressure. Rarefaction from front surface attenuates shock after about 1.5 nsec.

Fig. 5. Measurements with thin targets show that the shock is very unsteady at early times, regardless of the steadiness in the laser drive. This transient regime is not modeled well by the calculation.

Fig. 6. Measured shock velocities from targets without a CH ablation layer are not steady for a 30 or 60μm target thickness. Radiation from the ablation layer is heating the target and expanding the diagnostic steps before the shock reaches the rear of the target.
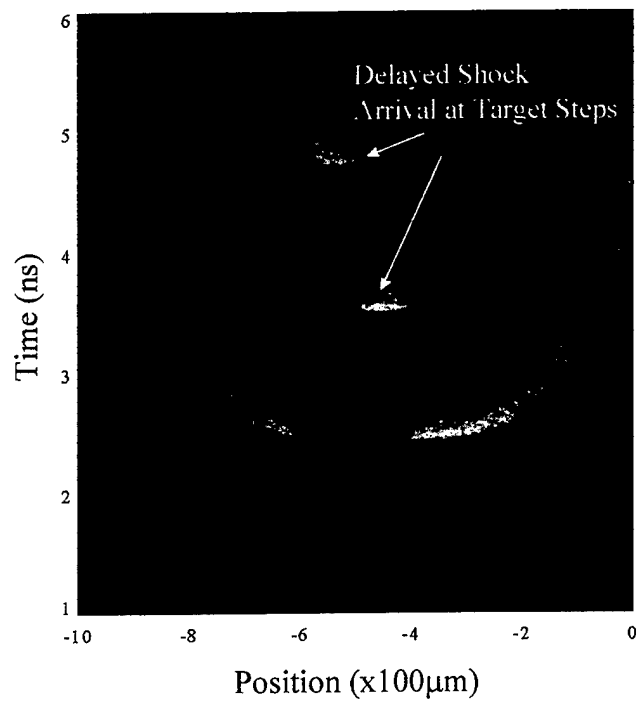
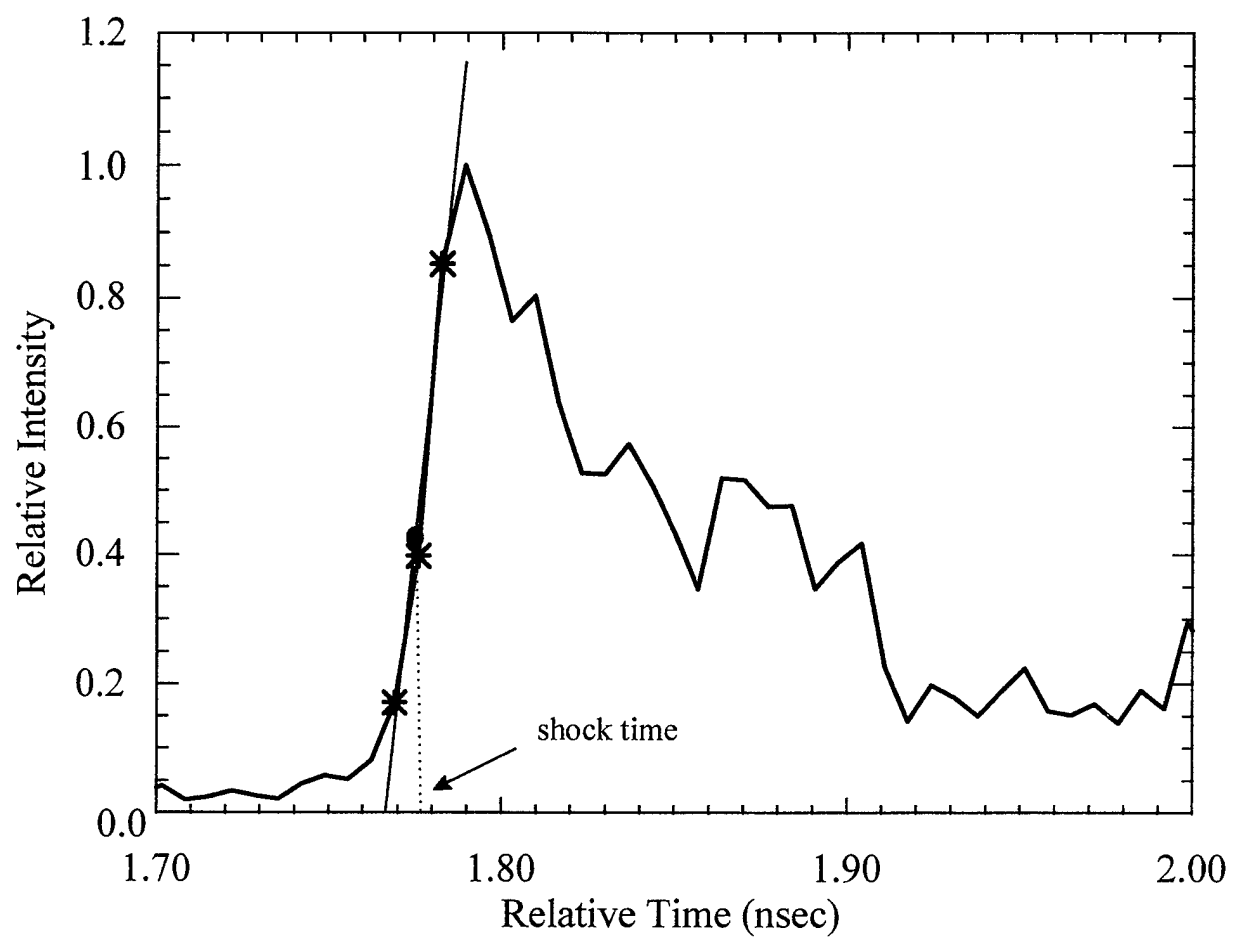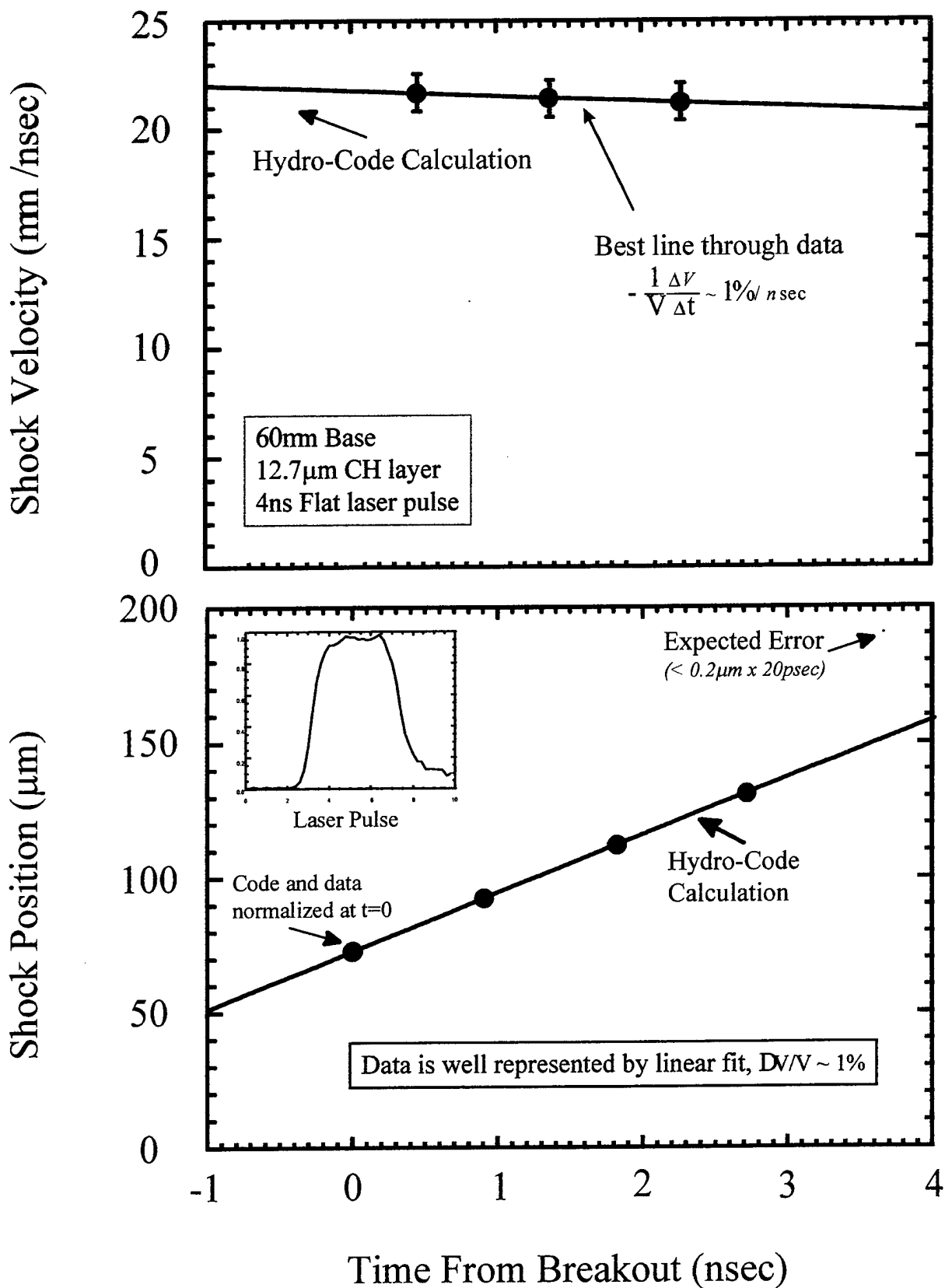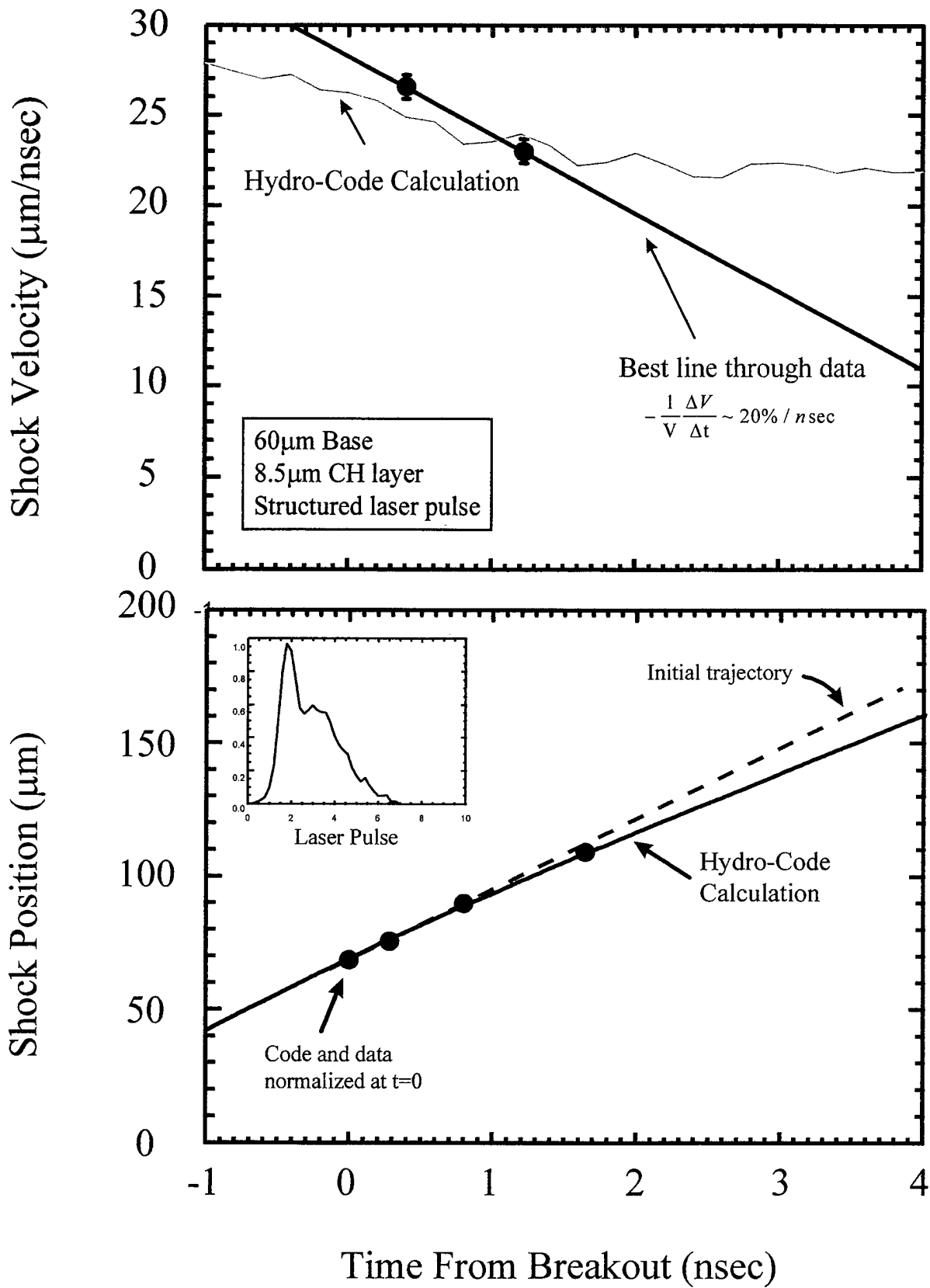Stepped Targets measure Shock Velocity
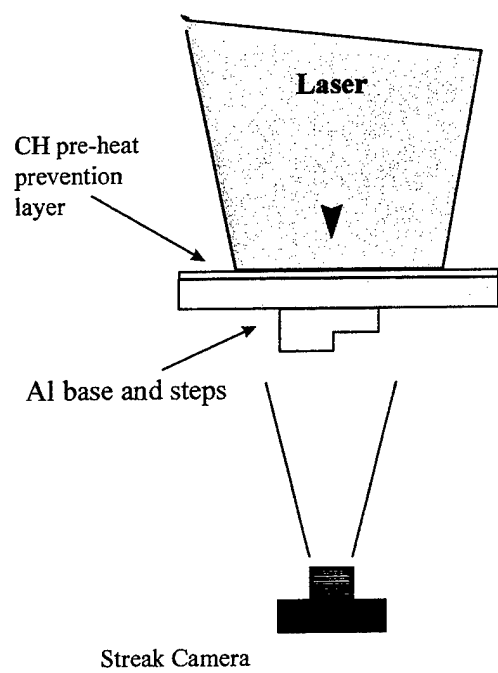
Typical Shock Data in Aluminum

Figure. 1

Figure 2.

Figure 3.

Figure 4.

Figure 5.

Figure 6.